J Mater Sci: Mater Med (2009) 20:1803–1814
DOI 10.1007/s10856-009-3754-9

Synthesis and characterisation of enhanced barrier polyurethane for encapsulation of implantable medical devices

Nima Roohpour · Jaroslaw M. Wasikiewicz · Deepen Paul · Pankaj Vadgama · Ihtesham U. Rehman

Received: 12 March 2009 / Accepted: 15 April 2009 / Published online: 28 April 2009

Abstract Polymeric membranes have been used as interfaces between implantable devices and biological tissues to operate as a protective barrier from water exchanging and to enhance biocompatibility. Polyurethanes have been used as biocompatible membranes for decades. In this study, copolymers of polyether urethane (PEU) with polydimethylsiloxane (PDMS) were synthesised with the goal of creating materials with low water permeability and high elasticity. PDMS was incorporated into polymer backbone as a part of the soft segment during polyurethane synthesis and physical properties as well as water permeability of resulting copolymer were studied in regard to PDMS content. Increase in PDMS content led to increase of microphase separation of the copolymer and corresponding increase in elastic modulus. Surface energy of the polymer was decreased by incorporating PDMS compared to unmodified PEU. PDMS in copolymer formed a hydrophobic surface which caused reduction in water permeability and water uptake of the membranes. Thus, PDMS containing polyurethane with its potent water resistant properties demonstrated a great promise for use as an implantable encapsulation material.

N. Roohpour · J. M. Wasikiewicz · D. Paul · P. Vadgama · I. U. Rehman (✉)
Interdisciplinary Research Centre in Biomedical Materials, School of Engineering and Material Sciences, Queen Mary University of London, Mile End Road, London E1 4NS, UK
e-mail: i.u.rehman@qmul.ac.uk

1 Introduction

The development of a new generation of implantable medical devices for both long-term and short-term use, requires rigorous application of protective barrier materials [1, 2]. The key requirement is to allow the device (i.e. biosensors, microelectronics and etc.) to operate consistent in the pressure of electrolyte medium of body (potentially corrosive). The ideal would be hermetic sealing using biocompatible barrier materials; to prevent any adverse interaction. Moreover, the material requires to be easily processed into the complex shape requiring the device to form a homogenous coating.

The need to protect both the device and biological tissues has restricted the range of useful materials. However, ceramics, glasses and metals were used in some applications, polymers are more popular [1–5]. Polymer coatings such as silicone rubber, PTFE, Parylene and epoxy were used to encapsulate the implantable devices [6–8]. However, these materials are biocompatible, they have limited abilities to protect the device from water ingress [4, 6, 9].

Polyether based polyurethane elastomers are currently used in a variety of blood and tissue contacting devices in biomedical application due to their biocompatibility and stability in biological environment together with their superior processability [10–12]. Despite their excellent mechanical properties and biocompatibility, the chemical structure and morphology of polyurethanes make them relatively permeable to gases and water [13–16].

Polyether–urethanes are permeable to both liquid water and water vapour. Surface properties, chain packing and phase separation are likely to affect permeability properties of polymeric membranes [14, 17, 18]. The driving force of water transmission process is the difference in the water concentration or vapour pressure between the two sides of

the membrane, which forms a concentration gradient within the membrane. Solubility of water in the film also plays an important role in diffusion process. The permeate water is first absorbed on the surface of the membrane on the side of highest water concentration. Then it diffuses across by dissolving in the membrane, which is usually called as activated diffusion. Upon arriving to the opposite surface of the membrane, which has a lower water concentration, it is desorbed and enters to the surrounding air space as vapour [19].

It is widely accepted that the slower the rate of water molecule absorption at the surface of membrane, rate of water transmission will also be lower through the membrane [16]. Thus, the rate of water transmission through a membrane can vary due to changes in surface hydrophilicity [15, 19]. The conventional approach, therefore to increasing water resistance of a polyurethane is chemical modification of the polymer by incorporation of a copolymer or preparing nano-composites by using nano particle additives [20].

Another important issue in implantable encapsulating materials is their stability in biological environment. Previous researches showed that polyether–urethanes underwent environmental stress cracking in vivo, and particularly when processed with residual stress [11]. The in vivo stability of polyurethanes has been increased by the addition of polydimethylsiloxane (PDMS) in the soft segment of the copolymer which also increases surface hydrophobicity [21, 22]. Considering these issues, it appears that PDMS has the potential of creating a balance between stability and water resistance in addition to biocompatibility and elastomeric properties [23].

Despite the noted advantages of PDMS, the intrinsic mechanical properties of PDMS oligomers and polymers are usually poor at room temperature. In order to develop useful properties such as mechanical properties, they have to be crosslinked or incorporated as a segment in an existing polymers [24–26]. The use of a small amount of PDMS is an effective way of modifying the polyurethanes' surface without dramatically changes bulk properties [27–29]. As PDMS posses low surface energy therefore, minimization of interfacial energy should be achieved by migration of low-energy chemical groups to the polymer–air interface [30, 31].

Analysis of surface has proved that silicon containing group (PDMS) are enriched at the air–polymer interface, and the Si enrichment gradually becomes less pronounced away from the interface toward the polymer bulk [32–34].

In this study PDMS containing polyurethane copolymers were synthesised via solution polymerization. Polytetramethylene oxide (PTMO) and hydroxyl terminated polydimethylsiloxane (PDMS) were used as the soft segment, and 4,4′-methylene diphenyl diisocyante (MDI) and 1,4-butanediol (BD) as the hard segment and chain extender respectively. Molecular structure, polymer morphology, surface properties, mechanical properties and water uptake of the synthetic polymers were studied in order to further explore the effect of PDMS on polyurethane properties. Furthermore, water transport of modified polyurethanes was compared with a clinically approved silicone rubber.

2 Experimental

2.1 Materials

Polytetramethylene oxide (PTMO, $M_n \sim 2000$, Sigma-Aldrich, UK) and polydimethylsiloxane (PDMS, $M_n \sim 2000$, Sigma-Aldrich, UK), were dehydrated at 80°C in vacuum for 24 h before use. The hydroxyl value of the polyols was corrected before use with method described by Stetzler et al. [35]. 1,4-butane diol (BD, Sigma-Aldrich, UK), 4,4′-methylene diphenyl diisocyanate (MDI, Sigma-Aldrich, UK) and dibutyltin dilaurate catalyst (DBTBL, Sigma-Aldrich, UK) were used as received. Tetrahydrofuran (THF, Sigma-Aldrich, UK) and dimethylformamide (DMF, Sigma-Aldrich,UK) were dried over molecular sieve (4 Å) before use.

2.2 Synthesis of polyurethane

Polyether polyurethane and PDMS containing polyurethanes were synthesised via two-steps; solution polymerization of PTMO, hydroxyl terminated PDMS, MDI and then chain extension with BD. The synthesis was carried out in a three-neck flask equipped with a stirrer, a nitrogen inlet and condenser guarded by a calcium chloride drying tube. The reaction was carried out at a molar ratio of PTMO:MDI:BD of 1:2:1. PDMS was added to the reactor in first step of the reaction which produces a polymer with higher molecular weight and homogeneous structure [36]. The temperature of the reaction in the first step was kept at 50°C until all the soft segment was dissolved in THF:DMF(1:1) mixed solvent. The MDI was also dissolved in the mixed solvent, but added drop-wise to the reactor. The temperature was gradually increased to 80°C and maintained for 1 h to form the prepolymer. The prepolymer was chain extended using BD at 120°C for 4 h. Reaction mixture was cooled down to room temperature and the copolymer was precipitated into propanol/water (1:1) solution, then washed with methanol and water several times, filtered and dried in a vacuum oven at 80°C for 24 h.

2.3 Preparation of membranes

Polyurethane film samples about 0.5–2 mm thick were cast on Petri dishes using 5–10% polyurethane solution (w/v) in THF. The Petri dishes were covered with lid, and films dried at room temperature for 72 h. The dried film was then placed in water for an hour before peeling the film off from the Petri dishes. The film was dried under vacuum at 0.1 torr and 80°C for 24 h before testing. Obtained films were examined under light microscope to ensure that there are no air bubbles or pinholes.

Silicone rubber (MED-4211) was purchased from NuSil, USA (Polymer Technology, UK) and cured according to the manufacturer recommendation.

2.4 Characterisation

2.4.1 NMR

Synthetic materials were characterised with proton (^{1}H) nuclear magnetic resonance (Burker AV 400 MHz) using $CDCl_3$ as a solvent (Burker Analytik GmbH, Germany).

2.4.2 FTIR

FTIR spectra of the synthesised polymers were obtained using a Nicolet 8700 FTIR spectrometer (Thermo Electron Corporation, UK), where the polymer sample films were cast on the KBr crystal to obtain spectra. Spectra were recorded in the mid infrared region (4000–400 cm^{-1}) at 4 cm^{-1} resolution and averaging 128 numbers of scans. The spectra data were acquired using OMNIC 7.2 software.

ATR-FTIR spectra were also obtained using the same spectrometer in conjunction with an Attenuated Total Reflectance (ATR) accessory at room temperature. Data were collected on KRS-5 using a variable-angle ATR unit at a nominal incident angle of 45°. Samples were cut randomly from polymer films, cut to ATR crystal size and mounted on both sides of a trapezoid crystal.

2.4.3 Raman

Raman spectra of the samples were recorded using a Nicolet Almega XR dispersive Raman spectrophotometer (Thermo Fisher Scientific, Madison Wisconsin, USA), equipped with a 785 nm laser. All the spectra were collected in the range 3430–100 cm^{-1} using a $\times 10$ objectives and over an average of 128 scans, 1 s exposure time at 4 cm^{-1} resolution.

2.4.4 Dynamic light scattering

Molecular weights of the polymers were obtained by using Zetasizer, nanoseries analyzer (ZS, Malvern Instruments Ltd. Worcestershire, UK) at 25°C using light scattering method according to the refractive index of the polyurethane [37]. Polymer solutions in THF with different concentration were prepared in range of (0.02–0.0025 g/ml), and filtered using 0.2 μm PTFE filter.

2.4.5 Mechanical testing

A tensile strength test was performed using an Instron Universal Testing machine (model 5584,Instron Co., UK) equipped with a 10 N load cell at room temperature. Dog bone shape specimens were cut from cast films using an ASTM D638 standard punch. The thickness of the films was between 0.1 and 0.3 mm. Specimens were kept in a desiccator at room temperature 1 week before testing. The specimens were stretched until break at a crosshead rate of 20 mm/min. Stress–strain curves were calculated, using the initial cross sectional area of the gauge section and the initial 4 mm gauge length. Young's modulus, E, was obtained by calculating the slope of the initial linear region of the stress–strain curve. Ultimate tensile strength (the maximum stress achieved prior to rupture) and percent elongation at break (the strain at rupture) were also obtained from the stress–strain curves.

2.4.6 Differential scanning calorimeter

A Mettler Toledo calorimeter DSC823 (UK) was used in this study. Samples were first heated at 10°C/min to 120°C and then cooled to −60°C and then reheated to 220°C at 10°C/min.

2.4.7 Dynamic mechanical analysis

Dynamic mechanical analysis (DMA) was carried out on a TA Instruments Q800 DMA at a dynamic frequency of 1 Hertz, and heating rate 2°C/min. The sample was a 0.3 mm thick solution cast film which was dried and aged over a week before testing.

2.4.8 Contact angle and surface energy

The contact angle of deionised water and α-Bromonaphthalene (Fluka) against the polymer surface was measured by the sessile drop method with a KSV CAM200 contact angle setup (KSV Instruments Ltd, Finland). The contact angle measurement was conducted at room temperature using liquid drops of 5 μl in size using a micro-litre syringe. The polymers were casted on a glass slide and further

Table 1 Surface energy calculation

$\gamma_S = \gamma_S^D + \gamma_S^P$	(1)
$\gamma_L = \gamma_L^D + \gamma_L^P$	(2)
$\gamma_{SL} = \gamma_S + \gamma_L - 2\left(\gamma_S^D \gamma_L^D\right)^{\frac{1}{2}} - 2\left(\gamma_S^P \gamma_L^P\right)^{\frac{1}{2}}$	(3)
$\gamma_S = \gamma_{SL} + \gamma_L Cos\theta$	(4)
$\gamma_L(1+\cos\theta) = 2\left(\gamma_S^D \gamma_L^D\right)^{\frac{1}{2}} + 2\left(\gamma_S^P \gamma_L^P\right)^{\frac{1}{2}}$	(5)

$\gamma_L =$ liquid-vapour tension; $\gamma_S =$ solid-vapour tension; $\gamma_{SL} =$ liquid-solid tension; $\gamma_S^D, \gamma_L^D =$ dispersion term; $\gamma_S^P, \gamma_L^P =$ polar term; $\theta =$ liquid–solid contact angle

Table 2 Surface energy of wetting liquid at 25°C [44]

Test liquid	$\gamma_L^P (\mathrm{mJ/m^2})$	$\gamma_L^D (\mathrm{mJ/m^2})$	$\gamma_L (\mathrm{mj/m^2})$
Water	51	21.6	72.6
α-Bromonaphthalene	0	44.6	44.6

dried in a vacuum oven before testing. The contact angles of both side of the drop were measured. Separate frames were collected every 2 s for 20 s and the mean contact angle was calculated using CAM software. The surface energy of the membrane was calculated by using the surface energy equations listed in Table 1 [38], and the surface energy of the solid calculated by the Eq. 1, and $\gamma_S^D$and γ_S^Pwere obtained from the Eq. 5 by testing the contact angle of the different liquids. The surface tension properties of the test liquids are listed in Table 2.

2.4.9 Water uptake

Polymer films were cut in to 60 mm × 10 mm × 0.3–0.4 mm and dried in a vacuum oven for 24 h to determine their dry weight (W_d). The water absorption of membranes was measured by immersion in deionised water at 37°C. The wet weight with different immersion times (W_t) was determined by wiping off the surface water with filter paper. The water absorption was then calculated by the following formula [39]:

$$W(\%) = \frac{W_t - W_d}{W_d} \times 100 \quad (6)$$

The average value of five readings from different samples is reported.

2.4.10 Water transmission

Liquid water permeability of the membranes (thickness ~0.25 mm) was determined at 37°C. Dry films were mounted and sealed on to open mouths of test bottles (r = 22.5 mm) containing hygroscopic agent (anhydrous copper sulphate, Sigma-Aldrich) and immersed in water for 1 week. Weighing the assembly allowed for determination of water transmission rate, from which permeability was calculated. A reference medical grade silicone rubber membrane was used as control. Data were compared using one-way analysis of variance (ANOVA) and P values ≤0.05 were considered statistically significant. Data are presented as mean ± standard deviation.

Water vapour transmission was determined by covering the open mouth of a conical flask (50 ml), filled with a known amount of deionised water (~10 ml), with polymeric membranes. Membranes were additionally sealed with Parafilm®. Measurement of water vapour transport, based on gravimetric determination of vaporised water, were taken daily for a period of 1 week. Each group of samples was measured simultaneously in triplicate and their average values were recorded.

3 Results

3.1 Synthesis of polymer

The control polyether polyurethane and PDMS containing polyether polyurethane were synthesised by the reaction of hydroxyl functional PTMO and PDMS with MDI and BDO in THF/DMF mixed solvent. A series of polyurethanes were synthesised by varying the ratio of PDMS to PTMO and hard segment. Synthesis conditions were optimised to obtain the maximum molecular weight of the polymer and together with maximum reaction yields are presented in Table 3.

3.2 Structure characterisation

The structure of the synthetic polymers was analysed using FTIR, Raman and NMR spectroscopy. The peak assignment of Raman and FTIR are tabulated in Table 4 and spectra of PDMS containing polyether–polyurethane are presented in Fig. 1a and b. The absorption bands around 3,330 cm^{-1} (H-bonded N–H stretch in urethane), 1,730 cm^{-1} (free urethane C=O), 1,704 cm^{-1} (H-bonded C=O) were assigned urethane linkage while the peak at 1,600 cm^{-1} assigns for C=C in benzene ring (this peak is stronger in Raman). The peak at 1,082 cm^{-1} shows the (C–O–C) stretch in polyether–polyurethane. The peaks at 1,258 cm^{-1} (bending of C–H in Si–CH_3), 1,100 cm^{-1} (–Si–O–Si– bending), 1,021 cm^{-1} (asymmetric stretching of Si–O–Si), 804 cm^{-1} (C–H in Si–CH_3) were assigned to the PDMS in copolymer. In Raman results, peaks at 503 cm^{-1} (Symmetric Si–O–Si), 718 cm^{-1}(Si–C stretch) are assigns for PDMS in polymer structure, and bands at 1,530, 1,303, 1,250 and 1,185 cm^{-1} are appearing after formation of urethane amide from polyurethane reaction [40].

^{1}H-NMR spectrum (Fig. 2) of the synthesized PDMS containing polyether–urethane revealed signals at

Table 3 Molecular weight and yield of reaction for various compositions of PDMS and PTMO based polyurethane copolymers

Sample ID	Hard segment (%)	PDMS (Wt%)	M_w	Yield of reaction (%)
PEU	23	0	81000	88
2PDMS–PEU	23	2	68400	85.4
10PDMS–PEU	23	10	45300	83.2
50PDMS–PEU	23	50	42300	74.8

Table 4 Bands assigned to FTIR and Raman spectroscopy of Polyurethane [12, 40, 46–51]

Wave number (cm^{-1})	Assignment	FTIR	Raman
3420	υ (N–H) free	s	w
3320	υ (N–H) H-bonded	s	w
2930	υ a(CH2)	s	s
2860	υ a(CH2)	s	s
1730–1732	Ester υ (C=O),urethane amideI υ (C=O)	s	m
1710–1702	υ (C=O) in Urethane	s	m
1600	υ (C=C in benzene ring(Ar))	m	s
1530	υ (Ar),urethane amide II, υ (C–N)+ δ(N–H)	s	m
1520	υ (C–N) + δ(N–H)	w	m
1450–1460	δ (CH2)	w	m
1340–1360	δ (CH2)(wagging)	m	w
1312	υ (C–N), υ (C–O)	s	m
1303	δ (CH),urethane amide III	m	s
1258	δ (CH) in Si–CH3	m	w
1250	Urethane amide III	s	s
1185	Urethane amide	w	s
1080	υ (C–O–C)	s	w
1020	υ a(Si–O–Si))	m	w
970–975	δ (CN)	w	m
960–965	w (CH2)	w	m
896–902	υ s(C–O–C)	w	m
860–865	δ(C–O–C), δ(C–C–C)	w	s
804	w (CH) in Si–CH3	m	w
718	υ (Si–C)	w	s
630–645	w (C–O)	w	m
503	υs (Si–O–Si)	w	s

υ Stretching, δ Bending, υa Asymetric stretching, υs Symmetric stretching, *Ar* Aromatic, *w* Wagging, *S* Strong, *M* Medium, *W* = Weak

$\delta = 0.14$ ppm (CH_3 from Si–CH_3), $\delta = 1.4$, 1.8, 3.6, 4.1 ppm (CH from 1, 4-butane diol and PTMO), $\delta = 3.8$, 7.2, 7.5 ppm (aromatic protons and benzyl protons on MDI) and also it exhibited a chemical shift at around 8.1 ppm, which is ascribed to protons on urethane amide group [24, 41, 42]. Raman, FTIR and NMR results are in good correlation with previously published data and confirmed the incorporation of PDMS in polyether–urethane.

3.3 Thermal analysis

Differential scanning calorimetery (DSC) and dynamic mechanical analysis (DMA) were used to investigate the effect of PDMS on polyurethane morphology. DSC thermograms of the polyether polyurethane and PDMS containing polyether–polyurethanes are illustrated in Fig. 3. PDMS in polyether–urethane increased the melting point of the soft segment which can be because of an increased phase separation due to the addition of PDMS.

DMA results also provided information on thermal transitions reflecting the morphological changes, supporting DSC results. In the PDMS containing copolymers, the main glass transition of the PTMO soft phase was higher than that of polyurethane control, suggesting complex microphase separation behaviour (Table 5).

3.4 Tensile test

Elastic modulus, ultimate tensile strength, and percent elongation at break were determined from stress–strain plots for each sample. The hard segment content of all samples was the same and all samples showed elastomeric behaviour in tests.

The results clearly demonstrate that, as the amount of PDMS in copolymer is increased, the ultimate tensile strength (UTS) and fail strain decreased (Fig. 4). The polyurethane with 2% PDMS showed the highest UTS between all the PDMS containing polymers. Generally, all materials were elastomeric with an elongation at break of over 300% which increased as the polyether content was increased. Sample with 2 wt% PDMS content showed the best similarity with control polyurethane in case of mechanical properties, which did not affect the mechanical properties of polyether–urethane.

3.5 Surface properties

The observation of surface segregation of the low surface energy segment (e.g. PDMS) has been widely reported in the siloxane containing block polyurethane systems. It has been shown that when a block copolymer is formed with PDMS and another copolymer, PDMS surface segregation will occur, if the other copolymer has a higher surface tension than PDMS [43].

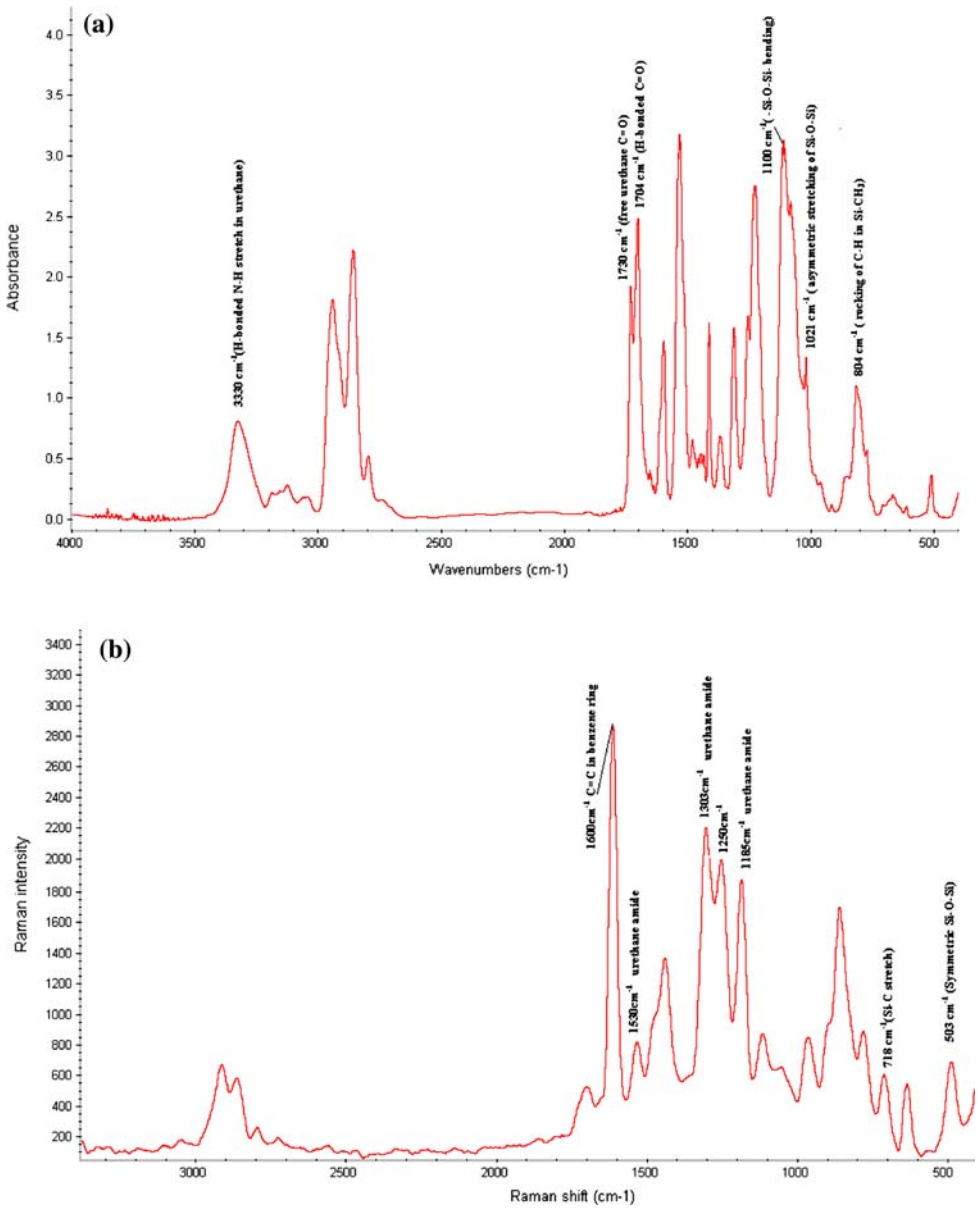

Fig. 1 **a** FTIR spectrum of PDMS (10 Wt%) containing polyether polyurethanes, **b** Raman spectrum of PDMS (10 Wt%) containing polyether polyurethanes

3.5.1 ATR-FTIR analysis

ATR-FTIR spectra of the 10% PDMS-polyether urethane (PEU) films were collected. Both the air interface and glass interfaces of the film were analysed to study the surface chemistry of the film at different interfaces. Results are showing the enrichment of PDMS at the air-interface. The peaks at 1,258 cm^{-1} (bending of C–H in $Si–CH_3$), 1,021 cm^{-1} (asymmetric stretching of Si–O–Si), 804 cm^{-1} (rocking of C–H in $Si–CH_3$) assigned to PDMS in the copolymer [43]. The intensity of these peaks at air interface shows a significant difference with glass interface (Fig. 5), which confirms the migration of PDMS segments to air interface resulting in reduced surface energy. Generally, molecules in polymeric films are arranged in a way to create minimum interfacial energy.

3.5.2 Contact angle measurement

The phenomenon of wetting of a solid by a liquid is better understood by studying the contact angle. Water contact angle is a representative of hydrophobicity or hydrophilicity of the surface. A water contact angle of 90° or more indicates a non wetting surface [44].

The results obtained are reported in Table 6. Hydrophobicity of polyurethane increases by incorporating PDMS resulting reduction of surface energy. The large water contact angles obtained for the PDMS containing

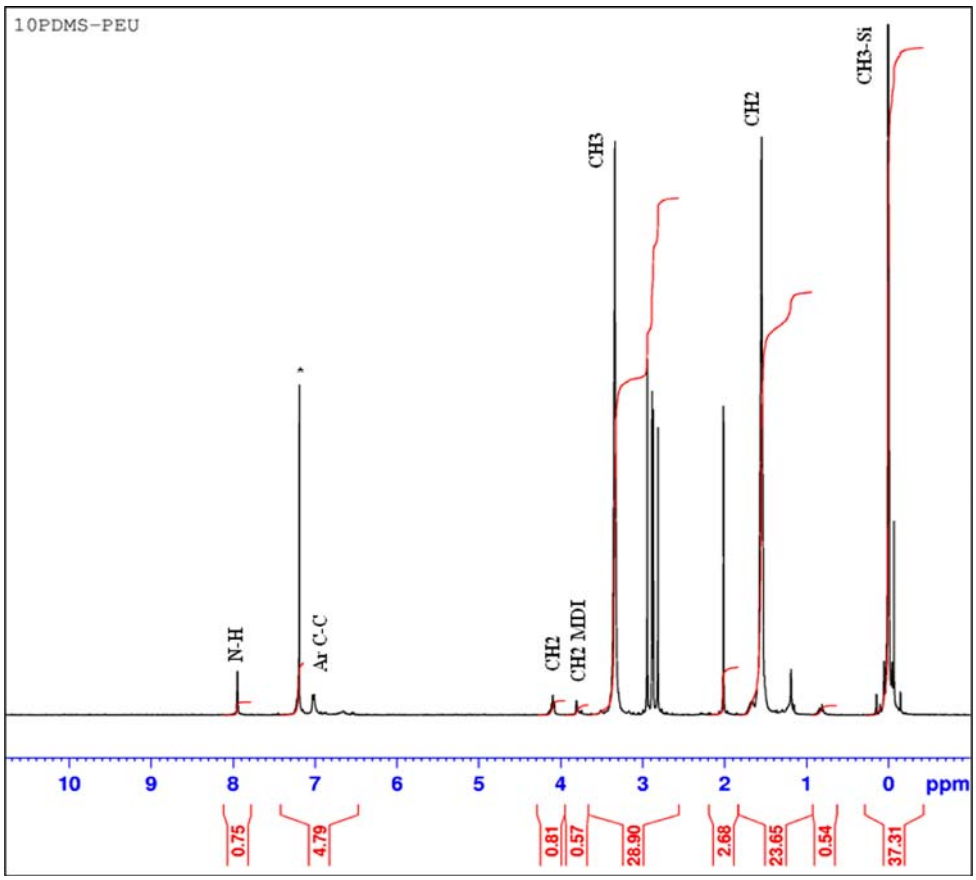

Fig. 2 ^{1}H NMR spectrum of PDMS (10 Wt%) containing polyether polyurethane (*$CDCl_3$)

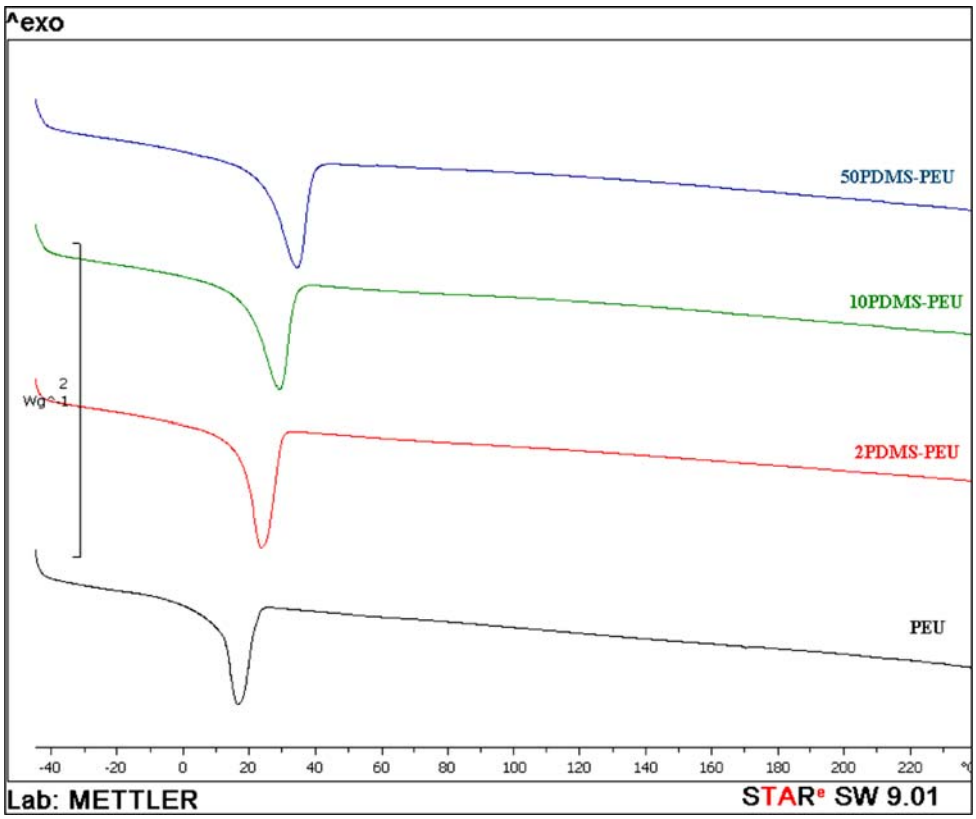

Fig. 3 DSC thermograms of polyether–urethane and PDMS containing copolymer

Table 5 Effect of PDMS content on glass transition temperature of polyether–urethane

Sample ID	T_g of PDMS (°C)*	T_g of PTMO (°C)*	T_{ms} (°C)**
PEU	–	−43	18
2PDMS–PEU	−102	−32	25
10 PDMS–PEU	−98	−30	28
50PDMS–PEU	−94	−25	34

* Measured by DMA

** Measured by DSC

polyurethane indicates the presence of a largely hydrophobic surface at air interface compared to the glass interface (2PDMS-R).

3.6 Water uptake

As shown in Fig. 6 the water uptake of polyurethane membranes decreased by increasing the PDMS content of the polymer. In first 12 h of immersion in water all PDMS containing membranes absorbed less water compared to an unmodified membrane. Absorption then increased with soaking time and levelled off after 36 h. The reduced water uptake of the membrane with 50 wt% PDMS shows the effect of the lower polarity PDMS segments compared with PTMO; while incorporation of 2 wt% PDMS had no significant effect.

3.7 Water permeability

Figures 7 and 8 are showing the water transport through polyurethane and silicone rubber membranes. Results are

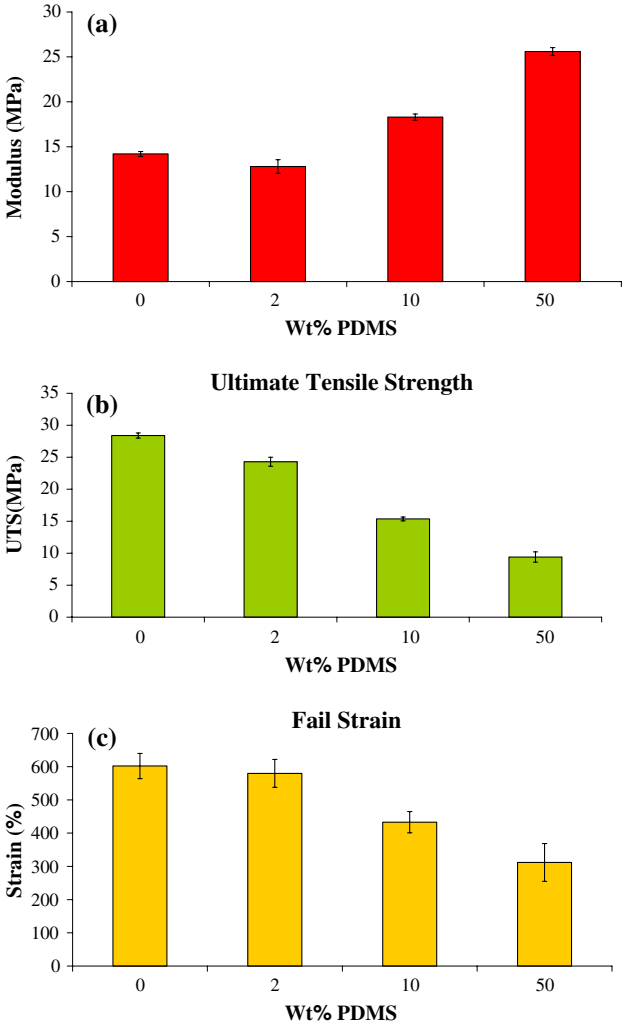

Fig. 4 The effect of PDMS content on **a** modulus, **b** ultimate tensile strength and **c** fail strain of polyether–urethane

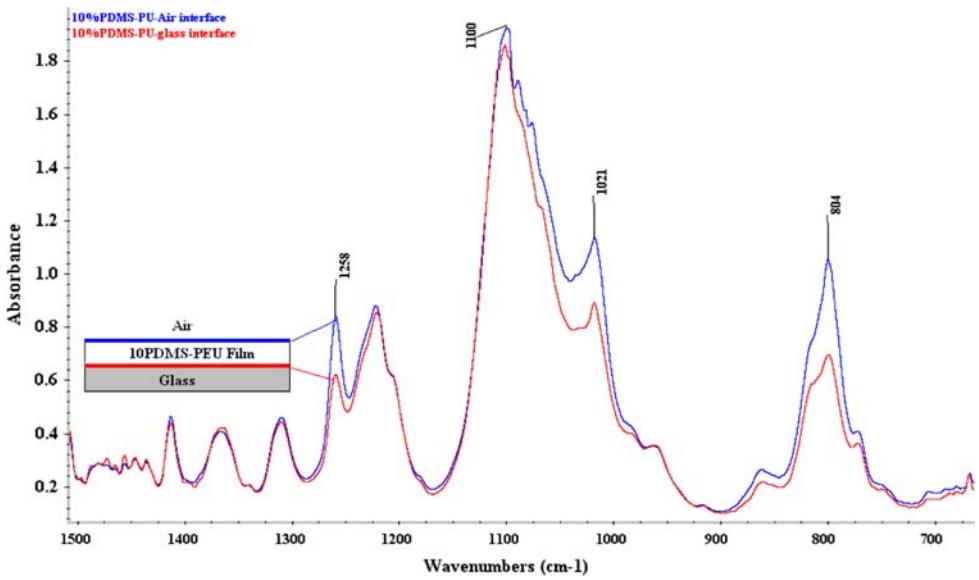

Fig. 5 ATR-FTIR spectrum of PDMS containing polyether–urethane (10 Wt%) collected on air and glass interface

Table 6 Contact angle and surface energy values (γ_S) of polyurethane membranes

Polymer	θ With water (°)	θ With α-bromonaphthalene (°)	γ_S^d (mNm^{-1})	γ_S^P (mNm^{-1})	γ_S (mNm^{-1})
PU	89.86 ± 1.62°	41.95 ± 2.04°	1.71	33.90	35.61
2PDMS–PEU	101.39 ± 1.16°	46.13 ± 1.81°	0.16	31.96	32.11
10PDMS–PEU	105.79 ± 2.30°	54.25 ± 2.11°	0.06	27.98	28.05
50PDMS-PEU	105.87 ± 3.16°	53.02 ± 3.76°	0.05	28.59	28.64
2PDMS–PEU-R	97.58 ± 1.72°	46.25 ± 3.49°	0.54	31.90	32.43

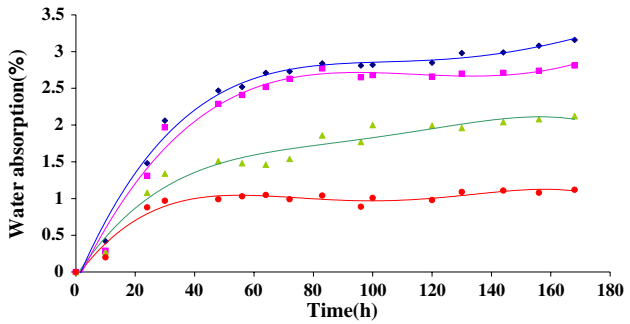

Fig. 6 Water uptake of polyurethane membranes and soaking time. PEU (◆); 2PDMS-PEU (■); 10PDMS-PEU (▲); 50PDMS-PEU (●)

showing less water transport through polyurethane series compared with silicone rubber which could be because of higher chain packing of polyurethane. Moreover, permeability of polyurethanes decreased with incorporation of PDMS. This may be due to the increased surface hydrophobicity which reduces the rate of water absorption at the surface of the membrane. It is clear from the results that even adding a small amount of PDMS in polyurethane structure led to decreased water permeability. The water permeability of all PDMS–PEU formulations were significantly lower than that of PEU alone ($P < 0.05$; Fig. 7) and interestingly the effect was independent of PDMS content. Although, PDMS has reduced the water transport in the first 24 h, the difference between modified and unmodified group were reduced by longer immersion (Fig. 7b). Water vapour permeability increased with incorporation of PDMS paradoxically (Fig. 8). The difference might be because of the role of the soft phase in permeation mechanism for H_2O.

4 Discussion

Here we reported the synthesis and characterisation of less water permeable polyurethane copolymers. These copolymers have several fascinating and promising properties, which can promote the use of silicone containing polyurethane in packaging implantable devices such as micro electronics. The excellent correlation between material hydrophobicity and PDMS content allows for control the permeability with respect to surface [16].

In respect to synthesis results, yield of the reaction and molecular weight of the polymers decreased by adding PDMS, which happened due to different solubility of the monomers in the solvent, however, since a mixed solvent system has shown improvement [24]. Results of NMR, FTIR and Raman spectra confirmed the formation of the PDMS–polyurethane copolymer and thermal analysis results are showing the phase separated nature of the copolymer. The observed differences in mechanical properties can be attributed to the ability of comacrodiol to interact with both urethane hard segments and siloxane soft segments. The weaker interactions between the PDMS containing soft segment and hard segments which caused by low polarity of PDMS segments explain the lower strength at breaking of polymer with higher PDMS content.

It is well known that mobility and electrostatic repulsion of polymer chains (especially soft segment in polyurethane) play important roles in water transport through polyurethane membranes. Generally, segmented polyurethanes can form segregated microphase structures in which crystalline hard segments are dispersed within a continuous soft segment matrix [12]. Due to the rigidity of the hard segment and its strong intermolecular forces, permeability of molecules linked mainly to the mobile soft segments, i.e. the rubbery state. Higher chain mobility is associated with a larger free volume in soft segment domains, which then facilitates the unhindered passage of water [16]. PDMS has increased separation of the two phases and consequently enhanced dispersion of hard and soft segment which can potentially reduce the chain mobility. On the other hand, water repulsive surface leads to the reduction of water absorption at surface of the polymer, and accordingly less water transport through the membrane occurs. In this study surface of membranes was modified in a way to reduce the water absorption by creating hydrophobic surface.

All polyurethane samples are showing less water permeability compared with silicone rubber which could be due to multiphase structure of the polyurethane and rigidity of the hard segment in polyurethane. The incorporation of

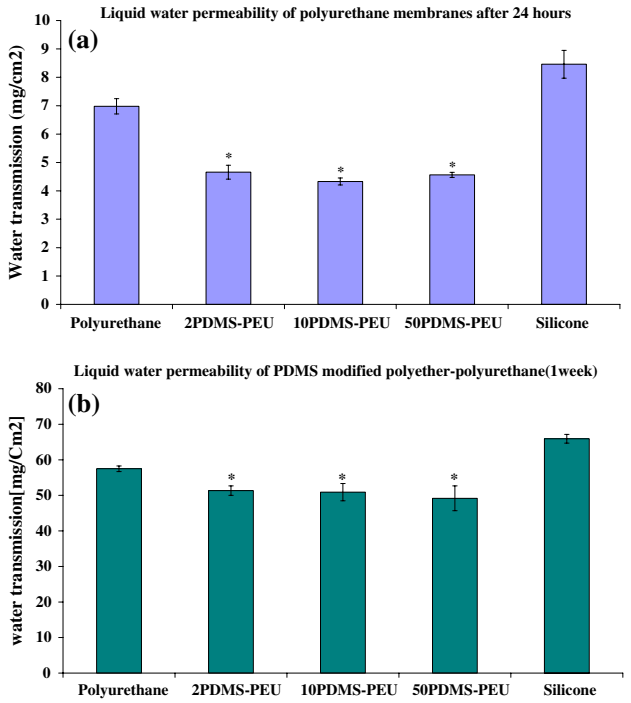

Fig. 7 Water transmission through PDMS containing polyurethane membranes in liquid water at 37°C, **a** after 24 h immersion; **b** after 7 days immersion in deionised water [9]. *P-value <0.05 compared to PEU; n = 3–4 samples per condition

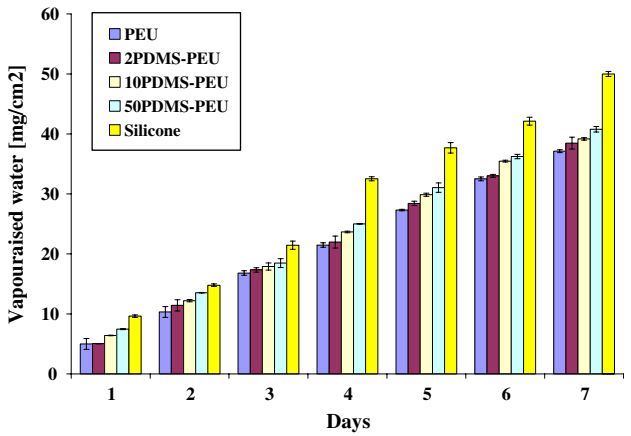

Fig. 8 Vapourised water transmission through PDMS modified polyether–urethane at 25°C

PDMS into the composition of the experimental copolymer not only resulted in a lower water transmission through membrane, but also a reduction in water uptake of the membrane, since PDMS is considered as a hyrophobe and non-polar material. Results of water permeability in liquid water are quite different with water vapour results. This might be because liquid transport is more sensitive to water repellence of the PDMS segments on membrane surface whereas gas phase water molecules are subject to fewer resistive forces. As the PDMS soft segment have much lower Tg than PTMO, the gas permeation should occur preferentially through the PDMS domains [17, 18, 45], as a result, vapour permeability increased by introducing more PDMS as soft segment. On the other hand, effect of PDMS on morphology of polymer due to different polarity and its incompatibility with other segments can reinforce the possibility of penetration of individual molecules such as gases.

5 Conclusion

As demonstrated in this report, a water resistant copolymer of PDMS–polyether urethane was synthesised whose physical and mechanical properties could be easily modified. The incorporation of PDMS in a polyurethane backbone introduced a water resistant membrane with an acceptable medical application background. Results of this research are encouraging the potential of PDMS modified polyurethane for application as a water resistant barrier for coating implantable devices with irregular shapes.

Acknowledgement We acknowledge generous support from European Union (Grant no IST-2002-1-001837–Healthy Aims).

References

1. Receveur RAM, Lindemans FW, de Rooij NF. Microsystem technologies for implantable applications. J Micromech Microeng. 2007;17:R50–80. doi:10.1088/0960-1317/17/5/R02.
2. Hodgins D, Bertsch A, Post N, Frischholz M, Volckaerts B, Spensley J, et al. Healthy aims: developing new medical implants and diagnostic equipment. IEEE Pervasive Comput. 2008;7:14–21. doi:10.1109/MPRV.2008.8.
3. Dario P, Carrozza MC, Benvenuto A, Menciassi A. Micro systems in biomedical applications? J Micromech Microeng. 2000;10:235–44. doi:10.1088/0960-1317/10/2/322.
4. Donaldson PEK. Encapsulating microelectronic implants in one-part silicone rubbers. Med Biol Eng Comput. 1989;27:93–4. doi:10.1007/BF02442177.
5. Hodgins D, Wasikiewicz JM, Grahn MF, Paul D, Roohpour N, Vadgama P, et al. Biocompatible materials developments for new medical implants. Med Device Technol. 2007;18:30–5.
6. Thil MA, Gerard B, Jarvis JC, Delbeke J. Two-way communication for programming and measurement in a miniature implantable stimulator. Med Biol Eng Comput. 2005;43:528–34. doi:10.1007/BF02344736.
7. Stieglitz T. Implantable microsystems for monitoring and neural rehabilitation, part I. Med Device Technol. 2001;12:2.
8. Rodger DC, Tai YC. Microelectronic packaging for retinal prostheses. IEEE Eng Med Biol Mag. 2005;24:52. doi:10.1109/MEMB.2005.1511500.
9. Wasikiewicz JM, Roohpour N, Paul D, Grahn M, Ateh D, Rehman I, et al. Polymeric barrier membranes for device packaging, diffusive control and biocompatibility. Appl Surf Sci. 2008;255:340–3. doi:10.1016/j.apsusc.2008.06.159.
10. Santerre JP, Woodhouse K, Laroche G, Labow RS. Understanding the biodegradation of polyurethanes: from classical

implants to tissue engineering materials. Biomaterials. 2005;26:7457–70. doi:10.1016/j.biomaterials.2005.05.079.
11. Stokes K, McVenes R, Anderson JM. Polyurethane elastomer biostability. J Biomater Appl. 1995;9:321–54.
12. Lamba NMK, Woodhouse KA, Cooper S. Polyurethane in biomedical application. London, UK: CRC; 1997.
13. McGee M, Szycher M, Turner SA, et al. Use of a composite biomer/butyl rubber/Biomer material to prevent transdiaphragmatic ater permeation during long term electrically actuated left vantricular device (LVAD) pumping. Trans Am Soc Artif Intern Organs. 1980;26:299.
14. Galland G, Lam TM. Permeability and diffusion of gases in segmented polyurethanes: structure-properties relations. J Appl Polym Sci. 1993;50:1041–58. doi:10.1002/app.1993.070500613.
15. William LEM, Hunke A Jr. Mass transport properties of co(polyether)polyurethane membranes II: permeability and sorption characteristics. J Pharm Sci. 1981;70:1313–8.
16. Yang MJ, Zhang Z, Hahn C, Laroche G, King MW, Guidoin R. Totally implantable artificial hearts and left ventricular assist devices: selecting impermeable polycarbonate urethane to manufacture ventricles. J Biomed Mater Res. 1999;48:13–23. doi:10.1002/(SICI)1097-4636(1999)48:1<13::AID-JBM4>3.0.CO;2-4.
17. Park HB, Kim CK, Lee YM. Gas separation properties of polysiloxane/polyether mixed soft segmented urethane urea membranes. J Membr Sci. 2002;204:257–69. doi:10.1016/S0376-7388(02)00048-0.
18. Gomes D, Peinemann KV, Nunes SP, Kujawski W, Kozakiewicz J. Gas transport properties of segmented poly(ether siloxane urethane urea) membranes. J Membr Sci. 2006;281:747–53. doi:10.1016/j.memsci.2006.05.002.
19. Yilgor I, Yilgor E. Hydrophilic polyurethaneurea membranes: influence of chemical composition on the water vapor permeation rates. Polymer (Guildf). 1999;40:5575–81. doi:10.1016/S0032-3861(98)00766-6.
20. Xu RJ, Manias E, Snyder AJ, Runt J. Low permeability biomedical polyurethane nanocomposites. J Biomed Mater Res A. 2003;64A:114–9. doi:10.1002/jbm.a.10377.
21. Martin DJ, Poole Warren LA, Gunatillake PA, McCarthy SJ, Meijs GF, Schindhelm K. Polydimethylsiloxane/polyether-mixed macrodiol-based polyurethane elastomers: biostability. Biomaterials. 2000;21:1021–9. doi:10.1016/S0142-9612(99)00271-9.
22. Mathur AB, Collier TO, Kao WJ, Wiggins M, Schubert MA, Hiltner A, et al. In vivo biocompatibility and biostability of modified polyurethanes. J Biomed Mater Res. 1997;36:246–57. doi:10.1002/(SICI)1097-4636(199708)36:2<246::AID-JBM14>3.0.CO;2-E.
23. Bernacca GM, O'Connor B, Williams DF, Wheatley DJ. Hydrodynamic function of polyurethane prosthetic heart valves. Biomaterials. 2002;23:45–50. doi:10.1016/S0142-9612(01)00077-1.
24. Wang LF, Ji Q, Glass TE, Ward TC, McGrath JE, Muggli M, et al. Synthesis and characterization of organosiloxane modified segmented polyether polyurethanes. Polymer (Guildf). 2000;41:5083–93. doi:10.1016/S0032-3861(99)00570-4.
25. Lin Y-H, Chou N-K, Chen K-F, Ho G-H, Chang C-H, Wang S-S, et al. Effect of soft segment length on properties of hydrophilic/hydrophobic polyurethanes. Polym Int. 2007;56:1415–22. doi:10.1002/pi.2291.
26. Ioan S, Grigorescu G, Stanciu A. Effect of segmented poly(ester-siloxane)urethanes compositional parameters on differential scanning calorimetry and dynamic-mechanical measurements. Eur Polym J. 2002;38:2295–303. doi:10.1016/S0014-3057(02)00108-8.
27. Adhikari R, Gunatillake PA, McCarthy SJ, Meijs GF. Mixed macrodiol-based siloxane polyurethanes: effect of the comacrodiol structure on properties and morphology. J Appl Polym Sci. 2000;78:1071–82.
28. Fan Q, Fang J, Chen Q, Yu X. Synthesis and properties of polyurethane modified with aminoethylaminopropyl poly (dimethyl siloxane). J Appl Polym Sci. 1999;74:2552–8.
29. Dou QZ, Wang CC, Cheng C, Han W, Thune PC, Ming WH. PDMS-modified polyurethane films with low water contact angle hysteresis. Macromol Chem Phys. 2006;207:2170–9. doi:10.1002/macp.200600375.
30. Queiroz DP, Botelho do Rego AM, de Pinho MN. Bi-soft segment polyurethane membranes: surface studies by X-ray photoelectron spectroscopy. J Membr Sci. 2006;281:239–44. doi:10.1016/j.memsci.2006.03.037.
31. Zhu Q, Feng S, Zhang C. Synthesis and thermal properties of polyurethane-polysiloxane crosslinked polymer networks. J Appl Polym Sci. 2003;90:310–5.
32. Wen J, Somorjai G, Lim F, Ward R. XPS study of surface composition of a segmented polyurethane block copolymer modified by PDMS end groups and its blends with phenoxy. Macromolecules. 1997;30:7206–13.
33. Liao SK, Jang SC, Lin MF. Phase behavior and mechanical properties of siloxane-urethane copolymer. J Polym Res. 2005;12:103–12. doi:10.1007/s10965-004-2501-7.
34. Meincken M, Berhane TA, Mallon PE. Tracking the hydrophobicity recovery of PDMS compounds using the adhesive force determined by AFM force distance measurements. Polymer (Guildf). 2005;46:203–8. doi:10.1016/j.polymer.2004.11.012.
35. Stetzler RS, Smullin CF. Determination of hydroxyl number of polyoxyalkylene ethers by acid-catalyzed acetylation. Anal Chem. 1962;34:194–5. doi:10.1021/ac60182a008.
36. Rochery M, Vroman I, TM Lam. Incorporation of poly(dimethylsiloxane) into poly(tetramethylene oxide) based polyurethanes: the effect of synthesis conditions on polymer properties. J Macromol Sci Part A Pure Appl Chem. 2003;A40:321–33. doi:10.1081/MA-120018117.
37. Theisen A, Johann C, Deacon MP, Harding SE. Refractive increment data-book for polymer and biomolecular scientists. Nottingham, UK: Nottingham University Press; 2000.
38. Kwok DY, Neumann AW. Contact angle measurements and contact angle interpretation. Adv Colloid Interface Sci. 1999;81:167–249. doi:10.1016/S0001-8686(98)00087-6.
39. Bai CY, Zhang XY, Dai JB, Zhang CY. Water resistance of the membranes for uv curable waterborne polyurethane dispersions. Prog Org Coat. 2007;59:331–6. doi:10.1016/j.porgcoat.2007.05.003.
40. Parnell S, Min K, Cakmak M. Kinetic studies of polyurethane polymerization with Raman spectroscopy. Polymer (Guildf). 2003;44:5137–44. doi:10.1016/S0032-3861(03)00468-3.
41. Madhavan K, Reddy BSR. Synthesis and characterization of poly(dimethylsiloxane-urethane) elastomers: effect of hard segments of polyurethane on morphological and mechanical properties. J Polym Sci Part A. 2006;44:2980–9.
42. Stanciu A, Airinei A, Timpu D, Ioanid A, Ioan C, Bulacovschi V. Polyurethane/polydimethylsiloxane segmented copolymers source. Eur Polym J. 1999;35:1959–65. doi:10.1016/S0014-3057(98)00294-8.
43. Rehman IU. Biodegradable polyurethanes; biodegradable low adherence films for the prevention of adhesions after surgery. J Biomater Appl. 1996;11:182–257.
44. Rochery M, Vroman I, Campagne C. Poly(tetramethylene oxide)-based polyurethane coating of polyester with poly(dimethylsiloxane)- and poly(tetramethylene oxide)-based polyurethane. J Industrial Textiles. 2006;35:227–38. doi:10.1177/1528083706055755.
45. Queiroz DP, Norberta de Pinho M. Structural characteristics, gas permeation properties of polydimethylsiloxane/poly(propylene oxide) urethane/urea bi-soft segment membranes. Polymer (Guildf). 2005;46:2346–53. doi:10.1016/j.polymer.2004.12.056.

46. Miller JA, Lin SB, Wang KK, Wu KS, Gibsson PE, Cooper SL. Properties of polyether-polyurethane block copolymers: effects of hard segment length distribution. Macromolecules. 1985;18:32–44. doi:10.1021/ma00143a005.
47. Ning L, De-Ning W, Sheng-kang Y. Hydrogen-bonding properties of segmented polyether poly(urethane urea) copolymer. Macromolecules. 1997;30:4405–9.
48. Mattia J, Painter P. A comparison of hydrogen bonding and order in a polyurethane and poly(urethane-urea) and their blends with poly(ethylene glycol). Macromolecules. 2007;40:1546–54. doi:10.1021/ma0626362.
49. Janik H, Palys B, Petrovic ZS. Multiphase-separated polyurethanes studied by micro-Raman spectroscopy. Macromol Rapid Commun. 2003;24:265–8. doi:10.1002/marc.200390039.
50. Kim H, Urban MW. Molecular level chain scission mechanisms of epoxy and urethane polymeric films exposed to UV/H_2O. Multidimensional spectroscopic studies. Langmuir. 2000;16:5382–90. doi:10.1021/la990619i.
51. Goheen SC, Saunders RM, Harvey SD, Olsen PC. Raman spectroscopy of 2-hydroxyethyl methacrylate-acrylamide copolymer using gamma irradiation for cross-linking. J Raman Spectrosc. 2006;37:1248–56. doi:10.1002/jrs.1543.